Article

Insights into Photodissociation Dynamics of Benzamide and Formanilide from ab Initio Calculations

Xue-Bo Chen, and Wei-Hai Fang

J. Am. Chem. Soc., **2004**, 126 (29), 8976-8980• DOI: 10.1021/ja0494858 • Publication Date (Web): 03 July 2004

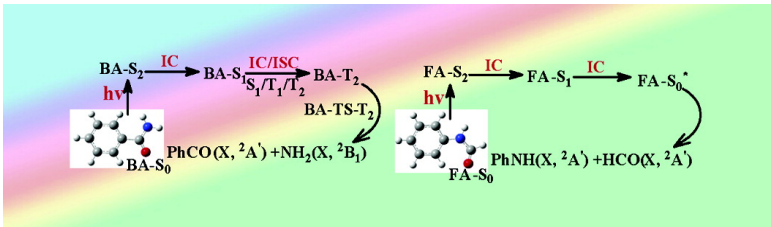

More About This Article

Additional resources and features associated with this article are available within the HTML version:

- Supporting Information
- Links to the 2 articles that cite this article, as of the time of this article download
- Access to high resolution figures
- Links to articles and content related to this article
- Copyright permission to reproduce figures and/or text from this article

View the Full Text HTML

J|A|C|S
ARTICLES
Published on Web 07/03/2004

Insights into Photodissociation Dynamics of Benzamide and Formanilide from ab Initio Calculations

Xue-Bo Chen and Wei-Hai Fang*

Contribution from the Department of Chemistry, Beijing Normal University, Beijing 100875, P. R. China

Received January 29, 2004; E-mail: Fangwh@bnu.edu.cn

Abstract: In the present study, the five lowest electronic states that control the UV photodissociation of formanilide and benzamide have been characterized using the complete active space self-consistent field theory. The mechanisms for the initial relaxation and subsequent dissociation processes have been determined on the basis of the calculated potential energy surfaces and their intersections. It was found that the $S_1/T_1/T_2$ three-surface intersection plays an important role in the photodissociation processes of benzamide. However, the dissociation behavior of formanilide and benzamide was found to be quite different from that for aliphatic amides. The present study provides several insights into the photodissociation dynamics of formanilide and benzamide.

Introduction

Photochemical triggers have been used to study fast events in protein folding.[1] How the peptide bond interacts with ultraviolet light has important implications in many fields such as modern structural biology.[1−3] Despite the wealth of experimental investigations done on the photochemistry of polypeptides and proteins, many aspects of their excited electronic states involved in the initial photoexcitation and subsequent processes are not well understood. As a first step toward exploring the photochemical behavior peptides, a series of simple amides—$HCONH_2$, CH_3CONH_2, and $CH_3CONHCH_3$[4−7]—have been investigated from a theoretical point of view. It was found that methyl substitution on the nitrogen or carbon atoms of the peptide bond has little influence on the rate of the peptide bond cleavage. This suggests the mechanism of photoinduced cleavage of the peptide bond is unchanged with the methyl substitution at many different positions. The planarity of the −CO−NH− group is a central feature linked to protein structure and function, and this has been discussed in a number of biochemistry textbooks. However, the n → π^* excitation of peptides results in a pyramidal −CO−NH− structure, which makes the cleavage of the peptide bond become easier. A phenyl substitution may have considerable influence on the nature of a peptide bond because of noticeable conjugation interaction. With the general aid to understand photoinduced breakage and formation of the peptide bond, formanilide (FA) and benzamide (BA), which have been a subject of numerous spectroscopic studies,[8−15] are investigated in this work to explore their photodissociation dynamics.

The five lowest electronic states that control the UV photodissociation of FA and BA have been characterized with complete active space self-consistent field theory (CASSCF) computations. The mechanisms for the initial relaxation and subsequent dissociation processes have been determined on the basis of the calculated potential energy surfaces and their intersections. The nature of the electronic states and the dissociation behavior of BA and FA was found to be significantly different from those for the amide molecules previously investigated. We believe that the results reported here provide several new insights into the photodissociation dynamics of formanilide and benzamide.

Computational Details

Stationary structures for FA and BA in the five lowest electronic states (S_0, S_1, S_2, T_1, and T_2) have been fully optimized by means of the complete active space self-consistent field (CASSCF) method employing the cc-pVDZ basis set. Once convergence has been reached, the harmonic frequencies were examined at this point to confirm the geometry obtained was a true minimum or first-order saddle point. The CASSCF calculations were carried out using the Gaussian 98 program

(1) Callender, R. H.; Dyer, R. B.; Gilmanshin, R.; Woodruff, W. H. *Annu. Rev. Phys. Chem.* **1998**, *49*, 173−202 and references therein.
(2) Cheng, Q.; Steinmetz, M. G.; Jayaraman, V. *J. Am. Chem. Soc.* **2002**, *124*, 7676−7677 and references therein.
(3) Wang, Y.; Hu, X. *J. Am. Chem. Soc.* **2002**, *124*, 8445−8451 and references therein.
(4) Liu, D.; Fang, W.-H.; Fu, X.-Y. *Chem. Phys. Lett.* **2000**, *325*, 86−92.
(5) Liu, D.; Fang, W.-H.; Lin, Z.-Y.; Fu, X.-Y. *J. Chem. Phys.* **2002**, *117*, 9241−9249.
(6) Chen, X.-B.; Fang, W.-H.; Fang, D.-C. *J. Am. Chem. Soc.* **2003**, *125*, 9689−9698.
(7) Chen, X.-B.; He, H.-Y.; Fang, W.-H. *J. Chin. Chem. Soc.* **2003**, *50*, 539−545.
(8) Manea, V. P.; Wilson, K. L.; Cable, J. R. *J. Am. Chem. Soc.* **1997**, 119, 2033−2039.
(9) Dickinson, J. A.; Hockridge, M. R.; Robertson, E. G.; Simons, J. P. *J. Phys. Chem. A* **1999**, *103*, 6938−6949.
(10) Robertson, E. G. *Chem. Phys. Lett.* **2000**, *325*, 299−307.
(11) Ullrich, S.; Tarczay, G.; Tong, X.; Dessent, C. E. H.; Muller-Dethlefs, K. *Phys. Chem. Chem. Phys.* **2001**, *3*, 5450−5458.
(12) Ullrich, S.; Tarczay, G.; Tong, X.; Dessent, C. E. H.; Muller-Dethlefs, K. *Angew. Chem., Int. Ed.* **2002**, *41*, 166−168 and references therein.
(13) Ullrich, S.; Tarczay, G.; Tong, X.; Dessent, C. E. H.; Muller-Dethlefs, K. *Chem. Phys. Lett.* **2002**, *351*, 121−127 and references therein.
(14) Kamran, G.; Werner, G.; Hiremagalur, J. *Curr. Med. Chem.* **2002**, *9*, 743.
(15) Takeuchi, H.; Sato, M.; Tsuji, T.; Takashima, H.; Egawa, T.; Konaka, S. *J. Mol. Struct.* **1999**, *485/486*, 175−181.

10.1021/ja0494858 CCC: $27.50

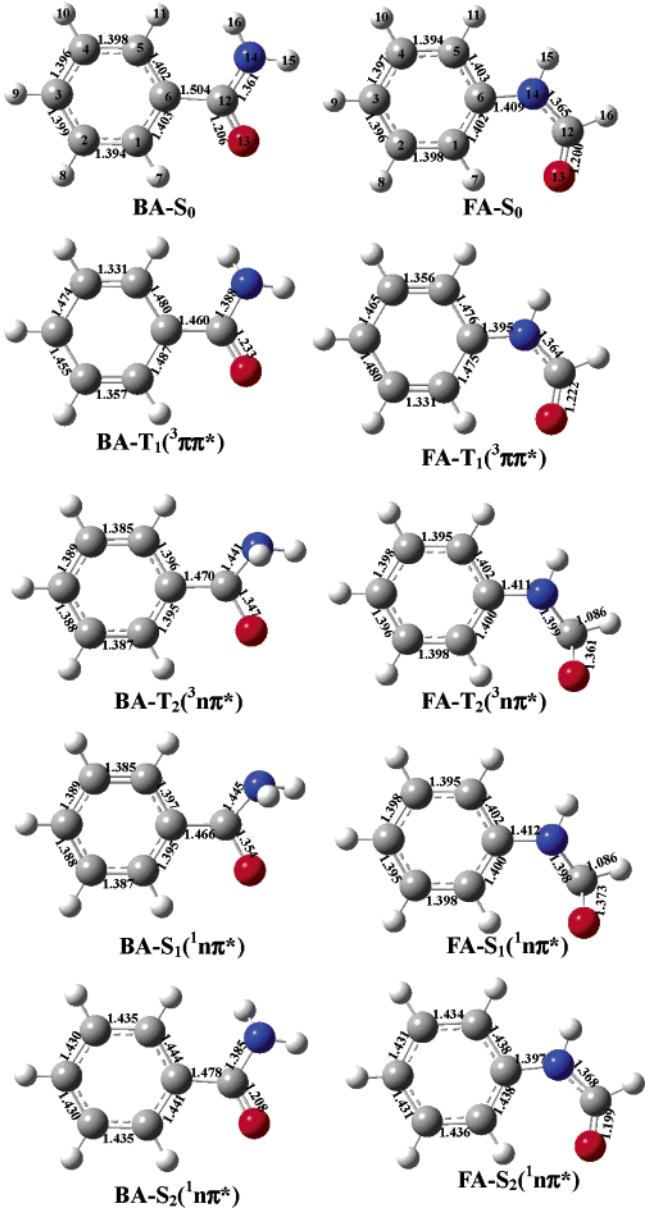

Figure 1. Schematic S_0, S_1, T_1, T_2, and S_2 minimum-energy structures for benzamide (BA) and formanilide (FA), along with the selected bond lengths (Å) and the atom-labeling scheme in the S_0 structures.

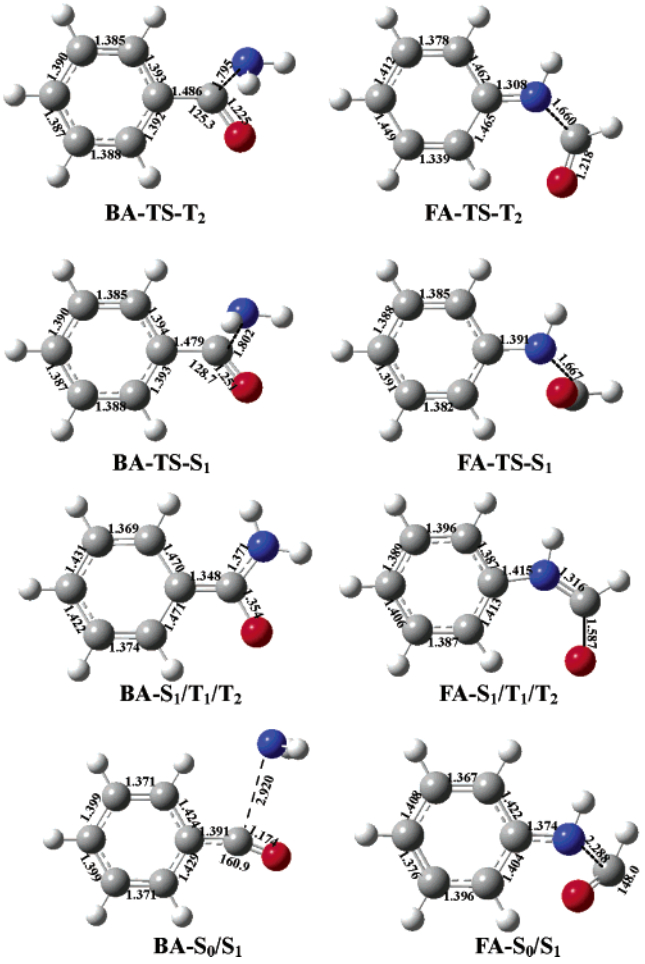

Figure 2. Schematic structures of transition states and intersection points for benzamide (BA) and formanilide (FA), along with the selected bond distances (Å).

package.[16] After preliminary CASSCF calculations with an active space of eight electrons in seven orbitals (referred to as CAS(8,7) hereafter) all stationary structures were optimized at the CAS(12,10) level of theory. For the equilibrium geometries on the S_0, S_1, S_2, T_1, and T_2 surfaces, 12 electrons and 10 orbitals were used that originate from the C=O π and π^* orbitals, the oxygen nonbonding orbital, the nitrogen $2p_z$ orbital, and three π and three π^* orbitals in the aromatic ring. This (12,10) active space was used to optimize the structures of the transition states (TS) for the C−N bond cleavage reactions with the lowest occupied π orbital in the aromatic ring replaced by the C−N σ orbital. In addition, one of the virtual orbitals in the active space had partial C−N σ^* character for the TS structures. Structural optimization of the surface intersection was performed with the state-averaged CASSCF method. Since the state-averaged calculation was very time-consuming, the (10,8) active space was used to search for the lowest energy point of the surface crossing seam. In this case, the lowest occupied π orbital in the aromatic ring and one of the π^* orbitals were excluded from the active space.

Results and Discussion

The optimized structures for the stationary and intersection points are schematically shown in Figures 1 and 2 with the atom-labeling scheme illustrated in the S_0 structures of FA and BA. The potential energy surfaces for the FA and BA dissociation processes are plotted in Figure 3, parts a and b, along with the CAS(12,10) relative energies. The structures and energies for all the stationary and intersection points reported in the present study are available in the Supporting Information.

The $\pi \rightarrow \pi^*$ transition has been assigned to the $S_0 \rightarrow S_1$ band of FA in previous spectroscopic studies.[9−13] The CAS(12,10)/cc-pVDZ calculations clearly show that the $^1\pi\pi^*$ state corresponds to the S_2 state for FA or BA. As listed in Table 1, the adiabatic excitation energy to the $^1\pi\pi^*$ state was predicted to be 102.7 and 101.2 kcal/mol for FA and BA, respectively, at the CAS(12,10) level of theory with the CAS(8,7) zero-point

(16) Frisch, M. J.; Trucks, G. W.; Schlegel, H. B.; Scuseria, G. E.; Robb, M. A.; Cheeseman, J. R.; Zakrzewski, V. G.; Montgomery, J. A., Jr.; Stratmann, R. E.; Burant, J. C.; Dapprich, S.; Millam, J. M.; Daniels, A. D.; Kudin, K. N.; Strain, M. C.; Farkas, O.; Tomasi, J.; Barone, V.; Cossi, M.; Cammi, R.; Mennucci, B.; Pomelli, C.; Adamo, C.; Clifford, S.; Ochterski, J.; Petersson, G. A.; Ayala, P. Y.; Cui, Q.; Morokuma, K.; Malick, D. K.; Rabuck, A. D.; Raghavachari, K.; Foresman, J. B.; Cioslowski, J.; Ortiz, J. V.; Stefanov, B. B.; Liu, G.; Liashenko, A.; Piskorz, P.; Komaromi, I.; Gomperts, R.; Martin, R. L.; Fox, D. J.; Keith, T.; Al-Laham, M. A.; Peng, C. Y.; Nanayakkara, A.; Gonzalez, C.; Challacombe, M.; Gill, P. M. W.; Johnson, B. G.; Chen, W.; Wong, M. W.; Andres, J. L.; Head-Gordon, M.; Replogle, E. S.; Pople, J. A. *Gaussian 98*, revision x.x; Gaussian, Inc.: Pittsburgh, PA, 1998.

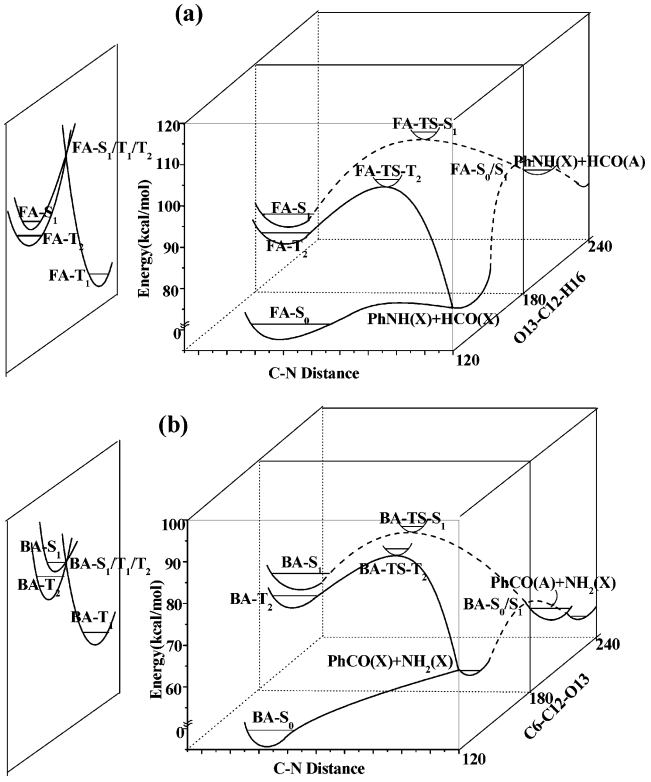

Figure 3. Schematic potential energy surfaces for formanilide (a) and benzamide (b) dissociations on different electronic states.

Table 1. Relative Energies (in kilocalories per mole) of the Stationary Structures

BA-S_0	0.0	FA-S_0	0.0
BA-T_1	69.7	FA-T_1	72.5
BA-T_2	82.1	FA-T_2	88.2
BA-S_1	86.0	FA-S_1	93.7
BA-S_2	101.2	FA-S_2	102.7
BA-TS-T_2	90.1	FA-TS-T_2	99.9
BA-TS-S_1	95.8	FA-TS-S_1	111.1

energy correction included. The origin of the $\pi \rightarrow \pi^*$ band was experimentally found to be $\sim$36 000 cm^{-1} (103 kcal/mol) for FA,[9] and this is very close to the CAS(12,10) calculated value. With respect to the S_0 zero-level point, the $^1n\pi^*$ state has a relative energy of 93.7 kcal/mol for FA and 86.0 kcal/mol for BA. It is evident that the $^1n\pi^*$ state should be the first excited singlet state (S_1) for the two molecules investigated here. Unlike the excited singlet state, the $^3\pi\pi^*$ state is the lowest triplet state (T_1) with relative energies of 72.5 kcal/mol for FA and 69.7 kcal/mol for BA. The $^3n\pi^*$ state, referred to as T_2, is energetically higher than the corresponding $^3\pi\pi^*$ state, but a few kilocalories per mole lower than the $^1n\pi^*$ state.

Unlike the origin of the $\pi \rightarrow \pi^*$ band that was experimentally assigned at $\sim$36 000 cm^{-1} (103 kcal/mol) for FA,[9] the relative energies of the other electronic states have not been determined experimentally for FA and BA. The band origins to the $^3n\pi^*$, $^1n\pi^*$, and $^1\pi\pi^*$ states of acetophenone ($PhCOCH_3$) have been experimentally observed to be 74, 78, and 101 kcal/mol, respectively.[17,18] Measurements of the sensitized phosphorescence spectra of jet-cooled acetophenone revealed that the $^3\pi\pi^*$ state is close to the $^3n\pi^*$ state in energy.[17] In comparison with acetophenone, the present calculations appear to provide a reasonable description on the nature and the relative energies of the four lowest-lying excited states of $PhCONH_2$ and HCONHPh. The two molecules have relatively large π conjugation systems, and the π and σ orbitals are well-separated in energy. Thus, the near-degenerate orbitals are included in the (12,10) active space of the present CASSCF calculations. This is one of the main reasons why the CAS(12,10) calculations can accurately predict the adiabatic excitation energies of $PhCONH_2$ and HCONHPh. The CASSCF calculations with six π electrons in six π orbitals predicts the $S_0 \rightarrow S_1$ transition energy to be 4.61 eV for toluene ($C_6H_5CH_3$),[19] which is close to the experimentally observed $S_0 \rightarrow S_1$ band origin of 4.65 eV. The $S_0 \rightarrow S_1$ band origin was observed to be 4.51 eV for phenol (C_6H_5OH), which was well-reproduced by the CASSCF calculations (4.64 eV) with eight π electrons in seven π orbitals.[20]

Structures of the five lowest electronic states for formanilide (FA-S_0, FA-S_1, FA-T_1, FA-S_2, and FA-T_2) and benzamide (BA-S_0, BA-S_1, BA-T_1, BA-S_2, and BA-T_2) have been optimized and confirmed to be minima by the CASSCF calculations. Similar to the ground state, the $^1\pi\pi^*$ excited state has a quasi-planar structure for FA and BA. As can be seen from bond parameters in Figure 1, the C−C bond lengths in the aromatic rings of FA and BA are nearly equal with a value of $\sim$1.40 Å in the ground state and $\sim$1.44 Å in the $^1\pi\pi^*$ state. The $\pi \rightarrow \pi^*$ excitation is mainly localized in the aromatic ring, and the lengthening of the C−C bonds in the ring exhibits characteristics of a $\pi \rightarrow \pi^*$ transition, where the aromatic ring attempts to reduce its π bonding character upon excitation. The C1−C2 and C4−C5 bond lengths in $^3\pi\pi^*$ are in the range of 1.33−1.36 Å, which indicates some double bond character, while the other C−C bonds in the aromatic ring are mainly of single bond character. Actually, the $^3\pi\pi^*$ state is a diradical with the two singly occupied electrons distributed on the C3 and C6 atoms. The C−C bond lengths of the ring are nearly unchanged upon the $n \rightarrow \pi^*$ excitation, but the C−O and C−N bonds are significantly lengthened from S_0 to $^1n\pi^*$ or $^3n\pi^*$. The $n \rightarrow \pi^*$ transition is mainly localized on the amide moiety for FA and BA.

As a general rule, regardless of which excited state is initially populated upon irradiation, the reactions proceed mainly along the ground or lowest excited state pathway. Thus, the surface intersection probably plays an important role in the photodissociation dynamics of a molecule. The T_1 and T_2 surface intersection (T_1/T_2) in the Franck−Condon (FC) region was optimized with the state-averaged CAS(10,8) approach, while the S_1 and T_1 crossing (S_1/T_1) structure was determined by using Slater determinants in the state-averaged CAS(10,8) calculations. It was found that T_1/T_2 and S_1/T_1 crossing points are indistinguishable in structure and the two crossing points are almost equal in energy. Actually, the S_1, T_1, and T_2 surfaces intersect at the same region, referred to as $S_1/T_1/T_2$. The $S_1/T_1/T_2$ structures for BA and FA, labeled by BA-$S_1/T_1/T_2$ and FA-$S_1/T_1/T_2$, respectively, are shown in Figure 2 along with selected CAS(10,8) bond parameters. The structure of the aromatic ring in BA-$S_1/T_1/T_2$ is similar to that in the T_1 minimum, while the structure of the carbonyl moiety of BA-$S_1/T_1/T_2$ is very close to that of the S_1 or T_2 minimum. Both S_1 and T_2 originate from

(17) Ohmori, N.; Suzuki, T.; Ito, M. *J. Phys. Chem.* **1988**, *92*, 1086−1094.
(18) Warren, J. A.; Bernstein, E. R. *J. Chem. Phys.* **1986**, *85*, 2365−1372.
(19) East, A. L. L.; Liu, H.; Lin, E. C. *J. Chem. Phys.* **2000**, *112*, 167.
(20) Fang, W.-H. *J. Chem. Phys.* **2000**, *112*, 1204.

the n → π^* transition, and they have similar structures. It is obvious that the $S_1/T_1/T_2$ three-surface intersection lies between the T_1 and S_1 minima for $PhCONH_2$. In comparison with FA-S_1 structure, the most striking changes in the FA-$S_1/T_1/T_2$ structure are associated with the C−O and C−N bond lengths. The $S_1/T_1/T_2$ three-surface intersection has also been found for PhCOR (R═H, CH_3, CH_3CH_2, and $CH_3CH_2CH_2$) molecules.[21]

The potential energy surfaces for the C−N bond cleavage on different electronic states are plotted in Figure 3, parts a and b. No potential barrier was found for the ground-state dissociation reactions. The reactions of $PhCONH_2(S_0)$ → $PhCO(\tilde{X}^2A')$ + $NH_2(\tilde{X}^2B_1)$ and $HCONHPh(S_0)$ → $PhNH(\tilde{X}^2A')$ + $HCO(\tilde{X}^2A')$ are endothermic by 62.9 and 61.7 kcal/mol, respectively. A transition state on the triplet pathway, referred to as BA-TS-T_2 in Figure 2, was determined by the CAS(12,10) optimization calculation. To confirm BA-TS-T_2 is the transition state on the reaction pathway from BA-T_2 to $PhCO(\tilde{X}^2A')$ + $NH_2(\tilde{X}^2B_1)$, the BA-TS-T_2 structure was re-optimized using the B3LYP/cc-pVDZ method and followed by the IRC calculations[22,23] at the same level of theory. A similar transition state of FA-TS-T_2 was confirmed to govern the T_2 dissociation of HCONHPh into $PhNH(\tilde{X}^2A')$ + $HCO(\tilde{X}^2A')$. The barrier height for the C−N bond scission along the T_2 pathway is 8.0 and 11.7 kcal/mol for BA and FA, respectively, at the CAS(12,10) level of theory with the CAS(8,7) zero-point energy correction included.

The 0−0 energy gap between $NH_2(\tilde{X}^2B_1)$ and $NH_2(\tilde{A}^2A_1)$ was determined to be about 29 kcal/mol,[24] while the adiabatic excitation energy from $PhCO(\tilde{X}^2A')$ to $PhCO(\tilde{A}^2A'')$ was predicted to be 10.5 kcal/mol by the CAS(9,8) calculations. Qualitatively, the S_1 dissociation of $PhCONH_2$ leads to formation of $PhCO(\tilde{A}^2A'')$ + $NH_2(\tilde{X}^2B_1)$ where the fragments are in the first excited state. A transition state was found on the S_1 pathway by the CAS(12,10) computations and was labeled by BA-TS-S_1 in Figure 2. The IRC calculations were done with the BA-TS-S_1 structure as the starting point. On the reactant side, BA-TS-S_1 was confirmed to connect $PhCONH_2$ in the S_1 state. However, on the product side, a problem of convergence was encountered during the state-specific CASSCF optimization of the IRC pathway. The S_0 and S_1 surfaces approach each other at a large C−N separation, and this results in the breakdown of the Born−Oppenheimer approximation. This implies that we have to consider the S_1 and S_0 surface intersection in this reaction. The geometry optimization for the intersection was carried out with the state-averaged CAS(10,8) method by searching for the lowest energy point of the surface crossing seam. The S_1 and S_0 surface intersection was found by the state-averaged optimization and is referred to as BA-S_1/S_0 hereafter. The S_1 C−N bond cleavage does not produce the fragments in the excited state, but yields the ground-state fragments of PhCO-$(\tilde{X}^2A')$ + $NH_2(\tilde{X}^2B_1)$, funneling through the BA-S_1/S_0 conical intersection. The S_1 direct dissociation of $PhCONH_2$ can be represented as BA-S_1 → BA-TS-S_1 → BA-S_1/S_0 → $PhCO(\tilde{X}^2A')$ + $NH_2(\tilde{X}^2B_1)$. With respect to the BA-S_1 zero-level energy, the transition state of BA-TS-S_1 has an energy of 9.8 kcal/mol and the BA-S_1/S_0 intersection is 13.8 kcal/mol lower in energy than the transition state. The same mechanism was found for the S_1 C−N bond scission of formanilide, which can be represented as FA-S_1 → FA-TS-S_1 → FA-S_1/S_0 → $PhNH(\tilde{X}^2A')$ + $HCO(\tilde{X}^2A')$. The geometric structures of FA-TS-S_1 and FA-S_1/S_0 are schematically shown in Figure 2. The barrier height was determined to be 17.4 kcal/mol for the S_1 C−N bond fission of formanilide. The FA-S_1/S_0 structure is 8.9 kcal/mol lower in energy than the transition state of FA-TS-S_1.

The $\pi \rightarrow \pi^*$ transition for FA or BA is mainly localized in the aromatic ring with a deep potential well, and the S_2 direct dissociation proceeds with little probability upon interaction with ultraviolet light. The FA and BA molecules in the S_2 state are almost planar, but they have nonplanar S_1 equilibrium structures. The normal modes are not only distorted but also mixed with each other in the S_2 → S_1 relaxation process. The frequency change and mode mixing make the S_2 → S_1 internal conversion (IC) occur with high efficiency through an increase in the vibrational part of the IC rate constant.[25] In addition, the energy difference between S_2 and S_1 is not large with a value of 9.0 kcal/mol for FA and 15.2 kcal/mol for BA. It is reasonable to expect that the FA and BA molecules in $S_2(^1\pi\pi^*)$ relax mainly to the $S_1(^1n\pi^*)$ state via the S_2 and S_1 vibronic interaction instead of radiation processes.

After relaxation to the S_1 state, the BA molecules are left with sufficient internal energies to overcome the barrier (9.8 kcal/mol) to the C−N bond cleavage along the S_1 pathway. However, the BA-$S_1/T_1/T_2$ intersection is only 1.3 kcal/mol in energy higher than the BA-S_1 minimum, and the S_1 → T_1 intersystem crossing (ISC) followed by the T_1 → T_2 IC via the BA-$S_1/T_1/T_2$ intersection is favorable from an energetic viewpoint. The difference in the S_1 and $S_1/T_1/T_2$ structures is small for BA, which originates from a redistribution of the conjugation π electrons. The BA molecules relax to the BA-$S_1/T_1/T_2$ intersection much more easily than to the BA-TS-S_1 structure upon photoexcitation, because of the initial excitation being localized in the aromatic ring. The S_1 → T_1 ISC takes place via the S_1/T_1 intersection with high efficiency, because of the strong first-order spin−orbit interaction.[26] The T_1/T_2 crossing point is a conical intersection between the T_1 and T_2 surfaces, and the time-scale for the T_1 → T_2 IC process via the conical intersection may be expected to be on the order of a vibrational period.[27] The T_1 state has been assigned as the $^3\pi\pi^*$ state that is unreactive, as discussed before. Besides the radiation pathway to the ground state by phosphorescence, the T_1 state of BA functions mainly as a relay and enables the S_1 → T_2 ISC to take place with a very high rate through the BA-$S_1/T_1/T_2$ intersection. Experimentally, it has been well-established that the magnitude of ISC rate constants are about 10^{11} s^{-1} for aromatic ketones (PhCOR, R = alkyl group).[26,28−31] These ISC rate constants are about 100-fold larger than the corresponding aliphatic ketones.[26] The above discussion gives us reason to

(21) Fang, W.-H.; Phillips, D. L. *ChemPhysChem* **2002**, *3*, 889−892.
(22) Gonzalez, C.; Schlegel, H. B. *J. Chem. Phys*. **1989**, *90*, 2154−2165.
(23) Gonzalez, C.; Schlegel, H. B. *J. Phys. Chem*. **1990**, *94*, 5523−5532.
(24) Herzberg, G. *Molecular Spectra and Molecular Structure III. Electronic Spectra and Electronic Structure of Polyatomic Molecules*; Prentice Hall: New York, 1966.
(25) Mebel, A. M.; Hayashi, M.; Liang, K. K.; Lin, S. H. *J. Phys. Chem. A* **1999**, *103*, 10674−10690 and references therein.
(26) Turro, N. J. *Modern Molecular Photochemistry*; University Science Books: Mill Valley, CA, 1991.
(27) Bernardi, F.; Olivucci, M.; Robb, M. A. *Chem. Soc. Rev*. **1996**, *25*, 321−328.
(28) Anderson, R. W.; Hochstrasser, R. M.; Lutz, H.; Scott, G. W. *J. Chem. Phys.* **1974**, *61*, 2500−2506.
(29) Morris, J. M.; Williams, D. F. *Chem. Phys. Lett*. **1974**, *25*, 312−314.
(30) Matsumoto, T.; Sato, M.; Hiroyama, S. *Chem. Phys. Lett*. **1972**, *13*, 13−15.
(31) El-Sayed, M. A.; Leyerle, R. *J. Chem. Phys.* **1975**, *62*, 1579−1580.

expect that the S_1 direct dissociation for $PhCONH_2$ is not in competition with ISC to the T_2 state.

Once in the T_2 state, the C−N bond cleavage takes place easily, because of a low barrier (8.0 kcal/mol) on this pathway. The mechanism of the UV photoinduced C−N bond fission for $PhCONH_2$ is summarized as follows:

$$\text{BA-}S_0 + h\nu \rightarrow \text{BA-}S_2 \xrightarrow{\text{IC}} \text{BA-}S_1 \xrightarrow[S_1/T_1/T_2]{\text{ISC/IC}} \text{BA-}T_2 \xrightarrow{\text{BA-TS-}T_2} PhCO(X^2A') + NH_2(X^2B_1)$$

This mechanism is quite different from those for CH_3CONH_2 and the related aliphatic amides,[6] where the C−N bond cleaves either along the S_1 pathway or on the T_1 surface as a result of the $S_1 \rightarrow T_1$ intersystem crossing.

Although the $S_1/T_1/T_2$ three-surface intersection was found for FA, the $S_1 \rightarrow T_1$ ISC takes place with great difficulty for HCONHPh. First, a very large change in the structure of the −CO−NH− moiety from the S_1 Franck−Condon geometry is required to reach the FA-$S_1/T_1/T_2$ intersection region. Second, the FA-$S_1/T_1/T_2$ intersection has a relatively high energy (22.6 kcal/mol with respect to the S_1 minimum). In view of the high relative energy of FA-$S_1/T_1/T_2$ and the large change needed from the S_1 FC geometry to reach the FA-$S_1/T_1/T_2$ structure, there is less probability that the intersystem crossing takes place via the FA-$S_1/T_1/T_2$ intersection for HCONHPh. In addition, the S_1 direct dissociation does not proceed easily, because of a barrier of 17.4 kcal/mol on the dissociation pathway. After the UV photoexcitation of HCONHPh, the main channel for HCONHPh to deactivate is internal conversion to the ground state followed by C−N dissociation to HCO + PhNH. The mechanism of the HCONHPh photodissociation is either different from that for $PhCONH_2$ or different from that for aliphatic amides.

Acknowledgment. This work was supported by grants from the National Natural Science Foundation of China (Grant No. 20233020) and from Ministry of Science and Technology of China (Grant No. 2002CB613406).

Supporting Information Available: Structures and energies for the stationary and intersection points reported in the present work. This material is available free of charge via the Internet at http://pubs.acs.org.

JA0494858